



The University of
Nottingham

UNITED KINGDOM · CHINA · MALAYSIA

Tomczynska, Magdalena M. and Choong, Gabriel Y.H. and De Focatiis, Davide S.A. and Grant, David M. and Parsons, Andrew J. (2016) Compounding and rheometry of PLA nanocomposites with coated and uncoated hydroxyapatite nanoplatelets. In: The Polymer Processing Society Conference 2015, 21-25 September 2015, Graz, Austria.

Access from the University of Nottingham repository:

<http://eprints.nottingham.ac.uk/39149/1/Paper%20Graz%20-%20M%20M%20Tomczynska%20v2.pdf>

Copyright and reuse:

The Nottingham ePrints service makes this work by researchers of the University of Nottingham available open access under the following conditions.

This article is made available under the University of Nottingham End User licence and may be reused according to the conditions of the licence. For more details see: http://eprints.nottingham.ac.uk/end_user_agreement.pdf

A note on versions:

The version presented here may differ from the published version or from the version of record. If you wish to cite this item you are advised to consult the publisher's version. Please see the repository url above for details on accessing the published version and note that access may require a subscription.

For more information, please contact eprints@nottingham.ac.uk

Compounding and rheometry of PLA nanocomposites with coated and uncoated hydroxyapatite nanoplatelets

Magdalena M. Tomczynska ^{a)}, Gabriel Y. H. Choong, Davide S. A. De Focatiis, David M. Grant and Andrew J. Parsons

Faculty of Engineering, University of Nottingham, Nottingham, NG7 2RD, UK.

^{a)} Corresponding author: Magdalena.Tomczynska@nottingham.ac.uk

Abstract. Polylactic acid and novel nanoplatelets of hydroxyapatite (HANP) were compounded in a laboratory scale twin-screw extruder and injection moulded to shape. The effect of HANP loading content, between 1 wt% and 10 wt%, and of HANP surface coating with tailored molecular dispersants, on the processability and rheological behaviour were investigated. Dispersion of HANP within the matrix system was determined qualitatively using transmission electron micrographs. Surface coating of HANP with dispersants was observed to change the state of HANP dispersion in the nanocomposites. This was also reflected in the changes of the nanocomposites' rheological response with the moduli of coated HANP systems increasing at lower frequencies.

INTRODUCTION

Biocompatible polymeric materials are an attractive alternative to metal implant devices used in medical procedures. Biodegradable polymer fracture fixation implants do not require a secondary operation to remove the device, but may require reinforcement in load-bearing applications. Commercially available medical devices consisting of biodegradable polymers such as polylactic acid have low strength. The addition of nanoplatelets to the matrix system is intended to reinforce the polymer and extend the current scope of application for polymer-based implants. Hydroxyapatite (HA) is one of the most promising bioresorbable nanofillers since it is the main inorganic constituent of bone and has the potential to deliver appropriate mechanical, bioactive and degradation properties for biomedical composites. HA *nanocomposites* are employed, rather than *microcomposites*, as their modulus was shown to be higher [1].

This work examines the influence of HANP loading content and of customised surface coating type on the processability, rheological response and HANP dispersion in the matrix. The novel bioresorbable materials are compounded by melt extrusion and formed by injection moulding, typically used in the manufacture of polymeric medical devices.

MATERIALS AND METHODS

Poly(L-co-D,L-lactide) (PLA), Resomer LR706S, was supplied by Evonik Industries AG, with a molar mass, M_w , of 445.9 kDa [2]. HANP were produced using a hydrothermal synthesis rig [3, 4, 5], and tailored molecular dispersants were synthesised consisting of either neat dodecenylsuccinic anhydride (DDSA) or short-chained PLA with an isosorbide head group (is-PLA) [6, 7]. Dispersants were added either separately to the compounder or coated onto the HANP *in situ* during particle synthesis [6, 7] and freeze dried.

LR706S was dried at 50 °C under vacuum for a minimum of 8 hours and transferred to a dry anaerobic glove box. The materials were dry mixed in the glove box to prevent moisture absorption causing excessive hydrolysis during melt processing [8].

Melt processing was performed using a HAAKE Minilab II twin-screw recirculating compounder fitted with co-rotating conical screws. Materials were compounded at 210 °C with a screw speed of 50 rpm for 15 min. Wall shear stress was measured during compounding via two pressure transducers located in a rectangular recirculation channel. Specimens were injection moulded with a HAAKE MiniJet injection moulding machine fitted with a custom Ø25 mm 1 mm thick disc mould. Compounded materials were extruded directly into the injection-moulding barrel at 205 °C with 800 bar pressure, and a mould temperature of 45 °C to produce disc specimens for further characterisation.

For rheometry, the extrudate from the compounder was subsequently compression moulded at 170 °C using a Daniels heated press with in-house moulds to produce isotropic Ø25 mm disc specimens. Dynamic rheological measurements were performed with an Anton Paar MCR302 rheometer fitted with a CTD620 temperature chamber using Ø25 mm parallel plates with a 0.5 mm gap size in air. Isothermal frequency sweeps were carried out at angular frequencies (ω) between 50 rad s⁻¹ and 1 rad s⁻¹ at low strain (1%), within the linear viscoelastic region, for temperatures from 90 °C to 210 °C. Mastercurves were produced by horizontally shifting the moduli in the frequency domain to a reference temperature of 180 °C.

Transmission Electron Microscopes (i) JEOL JEM 2200 MCO with a field emission gun (TEM-JEOL) at an accelerating voltage of 200 kV and 100 kV, and (ii) FEI TECNAI G2 BioTWIN with tungsten filament gun (TEM-FEI) at an accelerating voltage of 120 kV and 100 kV, were used to investigate the nanocomposite morphology. Sections ~100 nm thick were cut using a glass knife at room temperature and supported on copper grids.

RESULTS AND DISCUSSION

Compounding

Figure 1 shows the measurements of (a) screw torque (T) and (b) wall shear stress (τ_w) as a function of compounding time for up to 10 wt% of uncoated HANP. The addition of uncoated HANP to PLA leads to a significant decrease in T and τ_w , when compared to neat PLA. This implies that uncoated HANP have a plasticising effect on PLA, causing a significant decrease in melt viscosity [9].

Optical images of injection-moulded discs of unfilled PLA and HANP-PLA nanocomposites are shown in Fig. 2. The neat PLA disc was transparent; filler contents between 1 - 2.5 wt% of uncoated HANP produced translucent discs, whereas samples with concentrations >2.5 wt% were opaque. This suggests that PLA-HANP >2.5 wt% has agglomerate sizes predominantly in the microscale.

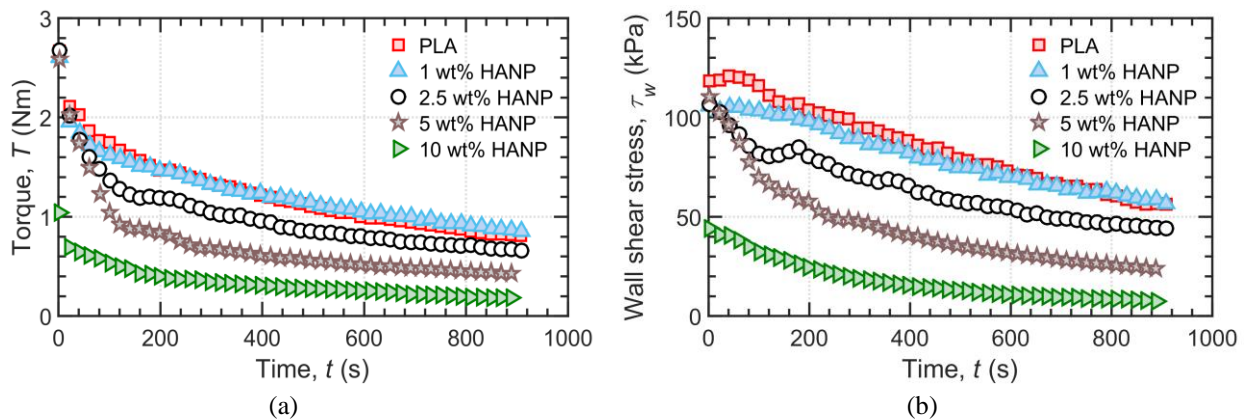


FIGURE 1. Influence of increasing content of raw HANP, 1 wt% to 10 wt%, in comparison to neat PLA: (a) torque, (b) wall shear stress. Data filtered with moving average of 5 points.

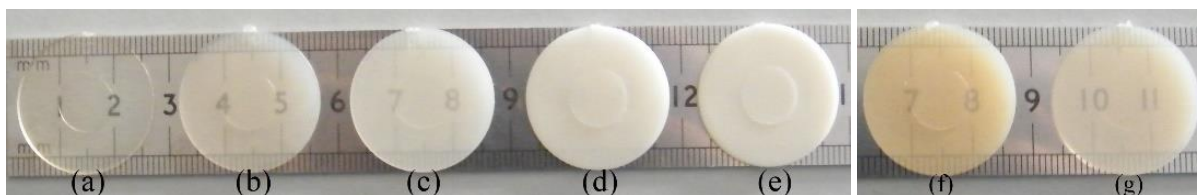


FIGURE 2. Injection moulded disc specimens - neat PLA (a); raw HANP-PLA: (b) 1 wt%, (c) 2.5 wt%, (d) 5 wt%, (e) 10 wt%; coated HANP-PLA: (f) 4.9 wt% is-PLA, (g) 2.8 wt% DDSA.

Figure 3(a) shows the melt compounding data for two types of *coated* HANP-PLA: (i) 4.9 wt% is-PLA coated and (ii) 2.8 wt% DDSA coated HANP (both with effective HANP of 2.5 wt%). During compounding, all coated HANP produced an *increase* in τ_w compared to PLA on its own. The injection-moulded discs of *coated* HANP-PLA were more translucent than the uncoated equivalent, as shown in Fig. 2(f)-(g), indicative of better dispersion and of the effectiveness of using tailored dispersants.

The importance of pre-coating dispersants onto nanoparticles in the hydrothermal synthesis rig was demonstrated in a comparative experiment where 2.5 wt% uncoated HANP and 0.28 wt% DDSA were added *separately* to the PLA in the compounder. This is equivalent in composition to the 2.8 wt% DDSA-coated HANP. This control experiment, illustrated in Fig. 3(b), displayed the same significant plasticising effect observed with the addition of uncoated HANP on their own. The increase in τ_w observed for 2.8 wt% DDSA-coated HANP relative to its control infers that the dispersant coating not only adheres to the HANP particles but also promotes HANP dispersion. This is further illustrated by TEM images shown in Fig. 4(a)-(f). The reduction of agglomerate size that can be observed in the coated systems (e) and (f) relative to the uncoated equivalent (b) is favourable for enhancing mechanical properties of polymer nanocomposites.

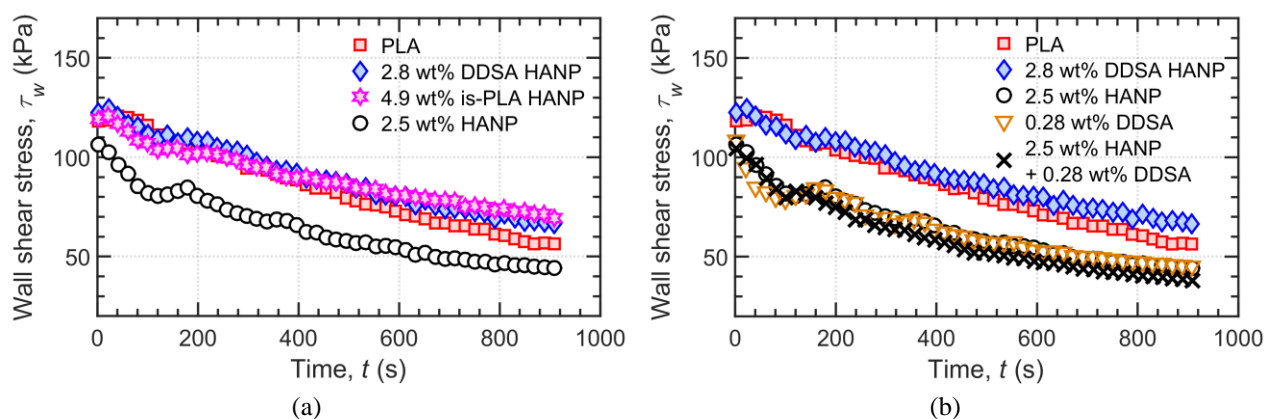


FIGURE 3. Comparison of melt compounding of PLA nanocomposites: (a) with raw and coated HANP, (b) *in situ* coated HANP and dispersants added separately onto nanoparticles. Data filtered with moving average of 5 points.

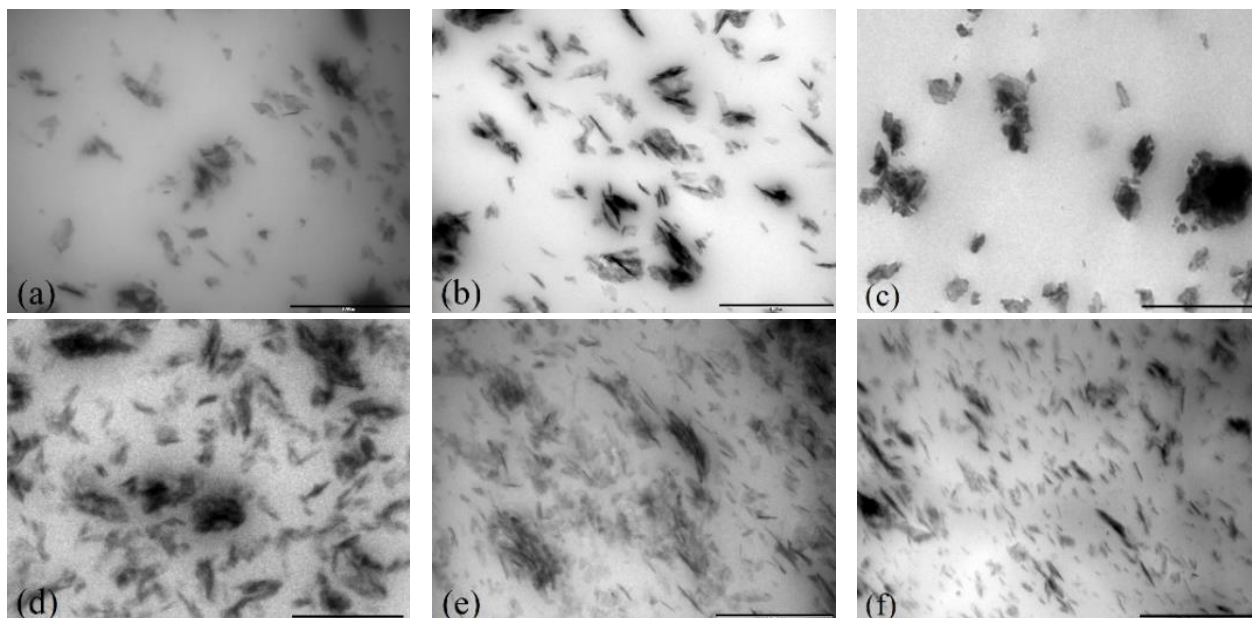


FIGURE 4. TEM images - raw PLA-HANP: (a) 1 wt%¹, (b) 2.5 wt%¹, (c) 5 wt%², (d) 10 wt%³; coated PLA-HANP: (e) 2.8 wt% DDSA¹, (f) 4.9 wt% is-PLA⁴. Scale bar 1 μm . TEM-FEI: (1) 100 kV, (2) 120 kV. TEM-JEOL: (3) 200 kV, (4) 100 kV.

Rheological Response

Figure 5 shows the rheological mastercurves of PLA, uncoated and coated PLA nanocomposites. In the uncoated system with 5 wt% HANP, the rheological response is similar to the pure polymer. For the 10 wt% uncoated system there is a reduction in moduli.

The coated HANP systems produced higher moduli at lower frequencies. The change in the low frequency response is plausibly related to the improved dispersion of HANP and decrease in HANP agglomerate size, as indicated by the TEM micrographs in Fig. 4. This suggests that rheometry could be used to provide insights into the material morphology, perhaps by linking to rheological models for particulate systems. However, it is acknowledged that further work is required to validate the technique.

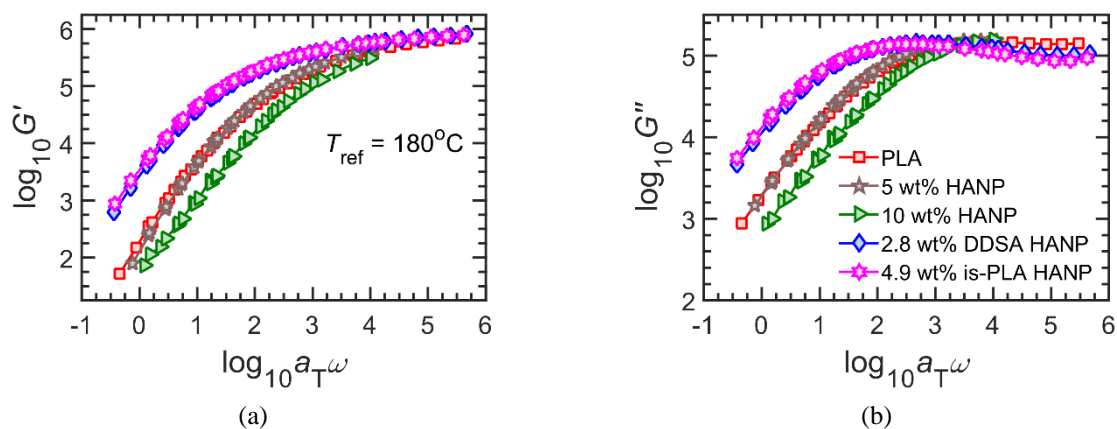


FIGURE 5. Mastercurves: (a) storage modulus (G') and (b) loss modulus (G''); for: neat PLA, raw HANP at 5 wt% and 10 wt%, and coated HANP: 2.8 wt% DDSA and 4.9 wt% is-PLA.

CONCLUSIONS

Nanocomposites were produced by melt compounding coated and uncoated HANP with PLA. The loading content of uncoated HANP and the type of dispersants were varied. The addition of uncoated HANP was found to decrease torque and wall shear stress during compounding. In contrast, the addition of coated HANP with tailored dispersants was found to increase wall shear stress during compounding. Coated HANP systems exhibited better dispersion of nanoparticles in the matrix as evidenced by TEM micrographs. The addition of uncoated HANP had no significant effect on the dynamic rheological moduli of the pure polymer, whereas an increase in the moduli of coated HANP systems were observed in the low frequency domain. The change in rheological response observed with coated HANP could be qualitatively related to the electron micrographs to infer HANP dispersion.

The reduction of agglomerate size with HANP functionalization is encouraging for reinforcing the base matrix. This work shows the importance of pre-coating tailored dispersants onto HANP in the hydrothermal synthesis rig to allow effective dispersion when processing PLA.

ACKNOWLEDGMENTS

This work was supported by grant EP/J017272/1 from the UK Engineering and Physical Sciences Research Council (EPSRC), and by a Travel Grant from the East Midlands Materials Society enabling attendance at the conference. Data created in support of this research is openly available at <http://dx.doi.org/10.17639/nott.14>.

REFERENCES

1. S.I.J. Wilberforce, C.E. Finlayson, S.M. Best & R.E. Cameron, *Polymer*, 52, 2883-2890 (2011).
2. G.Y.H. Choong, A.J. Parsons, D.M. Grant & D.S.A. De Focatiis, "Rheological techniques for determining degradation of polylactic acid in bioresorbable medical polymer systems", PPS Conference Proceedings 30, Polymer Processing Society, Cleveland, Ohio, 2014.
3. E. Lester, S.V.Y. Tang, A. Khlobystov, V.L. Rose, L. Buttery & C.J. Roberts, *CrystEngComm*, 15, 3256-3260 (2013).
4. Lester, E. & Azzopardi, B. (2005) Counter Current Mixing Device, Patent No. W/O 2005077505. Available at: <http://www.google.com/patents/WO2005077505A2> [Accessed 2 December 2015]
5. Lester, E. (2010) Hydroxyapatite material and methods of production, Patent No. W/O 2010122354. Available at: <http://google.com/patents/WO2010122354A1> [Accessed 2 December 2015].
6. F. Hild, K. Walton, M. Gimeno Fabra, E. Lester & D. Irvine, "Continuous, Single Stage Synthesis of Dispersant Included Nanoparticles", NanoBioTech-Montreux Conference, Montreux, Switzerland, 2014.
7. M. Gimeno-Fabra, F. Hild, P. Dunne, K. Walton, D. Grant, D. J. Irvine & E. Lester, *CrystEngComm*, 17, 6175-6182 (2015).
8. L.T. Lim, R. Auras & M. Rubino, *Progress in Polymer Science*, 33, 820-852 (2008).
9. M.E. Mackay, T.T. Dao, A. Tuteja, D.L. Ho, B. Van Horn, H.-C. Kim & C.J. Hawker, *Nature Materials*, 2, 762-766 (2003).